AD-A108 714 SCRIPPS INSTITUTION OF OCEANOGRAPHY LA JOLLA CA MARI--ETC F/G 17/1
HARDWARE DYNAMIC BEAMFORMING.(U)
AUG 80 W S HODGKISS, V C ANDERSON N00014-75-C-0749
UNCLASSIFIED MPL-U-42/80 NL

END
DATE FILMED
1-82
DTIC

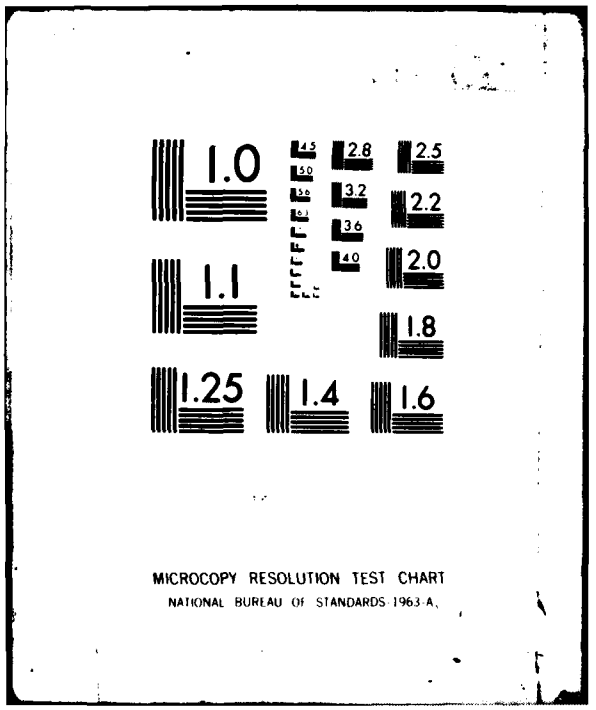
1.0
1.1
1.25
1.4
1.6
1.8
2.0
2.2
2.5
2.8
3.2
3.6
4.0
MICROCOPY RESOLUTION TEST CHART
NATIONAL BUREAU OF STANDARDS 1963-A

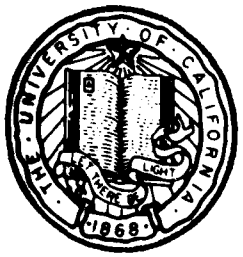

Hardware Dynamic Beamforming

W. S. Hodgkiss and V. C. Anderson

Supported by the Office of Naval Research Contract N00014-75-C-0749. Reproduction in whole or in part is permitted for any purpose of the United States Government. Approved for public release; distribution unlimited.

MPL-U-42/80

Reprinted from the Journal of the Acoustical Society of America, 69(4), pp. 1075-1083 (April 1981).

MARINE PHYSICAL LABORATORY
of the Scripps Institution of Oceanography
San Diego, California 92152

SECURITY CLASSIFICATION OF THIS PAGE *(When Data Entered)*

REPORT DOCUMENTATION PAGE		READ INSTRUCTIONS BEFORE COMPLETING FORM
1 REPORT NUMBER MPL-U-42/80	2. GOVT ACCESSION NO. AD-A108	3. RECIPIENT'S CATALOG NUMBER 714
4 TITLE *(and Subtitle)* HARDWARE DYNAMIC BEAMFORMING		5. TYPE OF REPORT & PERIOD COVERED Summary 6. PERFORMING ORG. REPORT NUMBER
7. AUTHOR(s) W. S. Hodgkiss and V. C. Anderson		8. CONTRACT OR GRANT NUMBER(s) N00014-75-C-0749
9 PERFORMING ORGANIZATION NAME AND ADDRESS University of California, San Diego, Marine Physical Laboratory of the Scripps Institution of Oceanography, San Diego, California 92152		10. PROGRAM ELEMENT, PROJECT, TASK AREA & WORK UNIT NUMBERS
11 CONTROLLING OFFICE NAME AND ADDRESS Office of Naval Research, Department of the Navy, Code 220, 800 N. Quincy Street, Arlington, Virginia 22217		12. REPORT DATE April 1981 13. NUMBER OF PAGES 8
14 MONITORING AGENCY NAME & ADDRESS*(if different from Controlling Office)*		15. SECURITY CLASS. *(of this report)* Unclassified 15a. DECLASSIFICATION/DOWNGRADING SCHEDULE

16. DISTRIBUTION STATEMENT *(of this Report)*

Approved for public release; distribution unlimited.

17. DISTRIBUTION STATEMENT *(of the abstract entered in Block 20, if different from Report)*

18. SUPPLEMENTARY NOTES

19. KEY WORDS *(Continue on reverse side if necessary and identify by block number)*

digital beamformer, element positions, steering direction

20. ABSTRACT *(Continue on reverse side if necessary and identify by block number)*

The hardware architecture of a programmable, time domain, digital beamformer built by the Marine Physical Laboratory is discussed. The Dynamic Beamformer permits the incorporation of slow changes in element positions and/or beam steering direction while carrying out the real-time formation of 1300 beams from 32 input sensors. The sensors are distributed in an arbitrary but known manner over a maximum aperture of 2 s in time delay, or 800 λ at the uppermost operating frequency of 400 Hz. Oversampling the sensor signals by a factor of 2.5 above the Nyquist rate is shown to permit the use

DD FORM 1 JAN 73 1473 EDITION OF 1 NOV 65 IS OBSOLETE
S/N 0102 LF 014 6601

SECURITY CLASSIFICATION OF THIS PAGE (When Data Entered)

of a simple, two-point linear interpolation filter to achieve the time-delay quantization intervals required. Element-(as opposed to beam-) level recording of the original sensor data provides a flexible and compact mechanism for postexperiment data analysis.

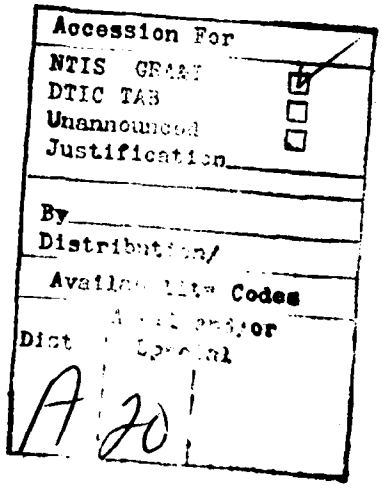

Hardware dynamic beamforming

W. S. Hodgkiss and V. C. Anderson

University of California, San Diego, Marine Physical Laboratory of the Scripps Institution of Oceanography, San Diego, California 92152

(Received 19 August 1980; accepted for publication 29 December 1980)

The hardware architecture of a programmable, time domain, digital beamformer built by the Marine Physical Laboratory is discussed. The Dynamic Beamformer permits the incorporation of slow changes in element positions and/or beam steering directions while carrying out the real-time formation of 1300 beams from 32 input sensors. The sensors are distributed in an arbitrary but known manner over a maximum aperture of 2 s in time delay, or 800 λ at the uppermost operating frequency of 400 Hz. Oversampling the sensor signals by a factor of 2.5 above the Nyquist rate is shown to permit the use of a simple, two-point linear interpolation filter to achieve the time-delay quantization intervals required. Element-(as opposed to beam-) level recording of the original sensor data provides a flexible and compact mechanism for postexperiment data analysis.

PACS numbers: 43.60.Gk, 43.60.Qv

INTRODUCTION

The concept of coherently combining the sensor outputs from a random array of freely drifting sonobuoys stimulated work by the Marine Physical Laboratory to fabricate a dynamically programmable beamformer. As conceived, the drifting sonobuoy array, depicted in Fig. 1, would be a sparse array with average element separations much larger than one-half wavelength at the frequencies of interest. The requirements imposed by this drifting, sparse array were the essence of Dynamic Beamformer design. Being a sparse array, the number of resolvable coherent combinations or beams formed from the individual sonobuoy sensor outputs would exceed by two or three orders of magnitude the number of elements themselves. Being a drifting array with time varying element locations, the beamforming time delays would need to be adjusted dynamically in order to accommodate the changing geometry.

This paper will focus on the design considerations and hardware architecture of the MPL Dynamic Beamformer and not dwell on the statistical theory of random arrays. The theory of random arrays, including the expected value and variance of the array spatial transfer function, the expected beam or power pattern, and the estimation of peak side-lobe level, is covered in detail elsewhere.[1-5]

Design considerations are based on the practical aspects of implementing the beamforming process. Section I develops the mathematics of time domain beamforming from an array whose elements are located arbitrarily in three-dimensional space. In addition, the number of beams which a sparse array must form to adequately probe the volume is discussed in general terms along with a specific example illustrating beam patterns from a 32-element, roughly planar, random array. Another important practical aspect relates to the effects of time-delay quantization and data interpolation for time domain beamforming. Section II outlines the specific hardware architecture of the MPL Dynamic Beamformer. Included is the format of multiplexing the sensor input data and blocking the beam output data. An example of the bearing response to a broadside sinusoidal signal also is provided as an illustration of performance degradation when data interpolation is not used. Section III comments on the data analysis flexibility available with this programmable beamformer. Lastly, Sec. IV provides a conclusion to the paper.

I. RANDOM ARRAY BEAMFORMING

The Dynamic Beamformer uses a time-delay-and-sum approach to coherently combine the element signals for a particular look direction. A large number of such combinations, or beams, must be generated in real time. The number, in fact, is so large that it becomes a significant factor in the beamformer architecture design. The statistical nature of the side lobes associated with a sparse, random array also must be recognized. Additionally, an important factor in the architecture design is the degree of quantization required in the time delays of the beamforming process. These topics will be pursued in this section.

A. Beamforming

The random arrays under consideration are composed of a three-dimensional distribution of equally weighted, omnidirectional sensors. Their spatial locations are specified in the Cartesian coordinate system of Fig. 2. Although the element positions are random variables, the assumption will be made that for any given array at a specified point in time, the $\mathbf{E}_n$ are known exactly.

The beamforming task consists of generating the waveform $b_m(t)$ (or its corresponding sampled sequence) for each desired steered beam direction $\mathbf{B}_m$. Each $b_m(t)$

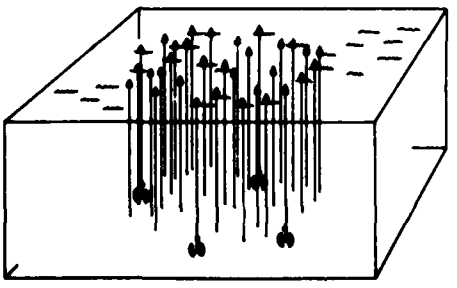

FIG. 1. Random sonobuoy array.

 0001-4966/81/041075-09$00.80

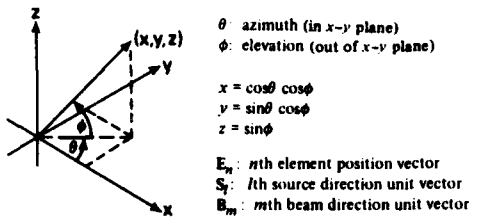

FIG. 2. Coordinate system definition and vector notation.

consists of the sum of suitably time delayed replicas of the individual element signals $e_n(t)$. The time delays compensate for the differential travel time differences between sensors for a signal from the desired beam direction.

Let the output of an element located at the origin of coordinates be $s(t)$. Under the assumption of plane-wave propagation, a source from direction $\mathbf{S}_l$ produces the following sensor outputs

$$e_n(t) = s[t + (\mathbf{E}_n \cdot \mathbf{S}_l)/c] \ , \tag{1}$$

where c is the speed of propagation ($c \simeq 1500$ m/s for acoustic waves in the ocean). Appropriately delaying the individual element signals to point a beam in the direction $\mathbf{B}_m$ yields the beamformer output

$$b_m(t) = \sum_{n=1}^{N} e_n\left(t - \frac{\mathbf{E}_n \cdot \mathbf{B}_m}{c}\right) , \tag{2}$$

$$= \sum_{n=1}^{N} s\left(t - \frac{\mathbf{E}_n \cdot (\mathbf{B}_m - \mathbf{S}_l)}{c}\right) . \tag{3}$$

The vectors involved in the scalar product of one component of (2) are illustrated in Fig. 3. Portrayed is an array of sensors in a plane-wave acoustic field where $\mathbf{B}_m = \mathbf{S}_l$.

The complexity of the beam formation process arises from the need to carry out the summation in (2) in real time for a large number of $\mathbf{B}_m$ directions or beams. In the Dynamic Beamformer, 32 element data inputs are transformed into 1300 beam data outputs. A distinguishing feature of the Dynamic Beamformer is that the

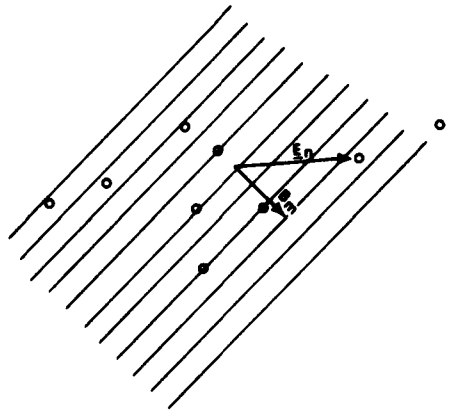

FIG. 3. Element time-delay calculation ($\mathbf{B}_m = \mathbf{S}_l$).

$\mathbf{B}_m$'s and $\mathbf{E}_n/c$'s are treated as dynamic variables and are allowed to change slowly during the transformation process. As indicated, fluctuations in either or both sound speed c and array element location $\mathbf{E}_n$ are mapped into variations within a time-delay coordinate system.

B. Number of beams required

It must be kept in mind that it is the projected aperture of the array in the beam steering direction ($\mathbf{B}_m$) and not the number of elements in the array which determines the beam pattern main-lobe width. Furthermore, the main-lobe width is dependent on the particular planar slice chosen in which the beam vector lies (e.g., horizontal versus vertical beamwidth). In one dimension, the nominal beamwidth is λ/L radians where λ is the wavelength of interest L is the projected aperture dimension.

As an example, consider a planar, circular array lying in the x–y plane of Fig. 2. Given an array whose diameter is D, the nominal horizontal beamwidth would be $\Delta\theta = \lambda/D$ rad. Thus the number of beams which would be required for full edgefire coverage would be $M = 2\pi/\Delta\theta = 2\pi(D/\lambda)$, where (D/λ) is the horizontal aperture dimension in wavelengths.

Consider now a spherical volumetric array whose diameter also is D. In this case, the nominal main-lobe width will be the same in any planar slice chosen in which the beam vector lies. Thus $\Delta\phi = \Delta\theta = \lambda/D$ rad and the corresponding solid angle beamwidth is $\Delta\Omega = \Delta\theta \cdot \Delta\phi = \lambda^2/D^2$ sr. In order to adequately probe all possible horizontal (θ) and vertical (ϕ) angles, the number of beams required would be $M = 4\pi/\Delta\Omega = 4\pi(D/\lambda)^2$.

Figure 4 plots these two values of M as a function of aperture dimension in wavelengths. In actual practice, the random arrays of interest are somewhere between circular planar and spherical volumetric. Further-

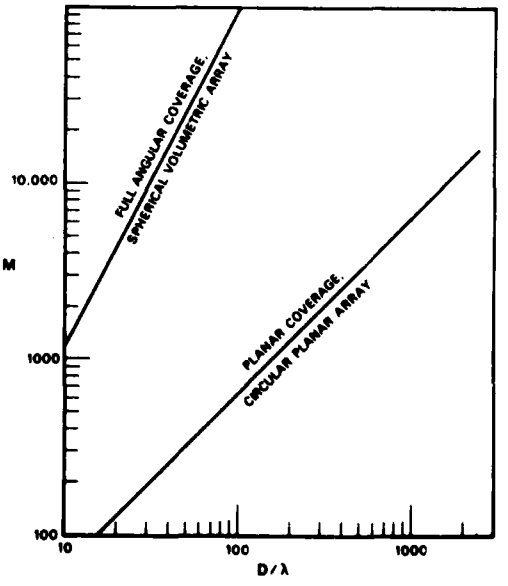

FIG. 4. Required number of beams.

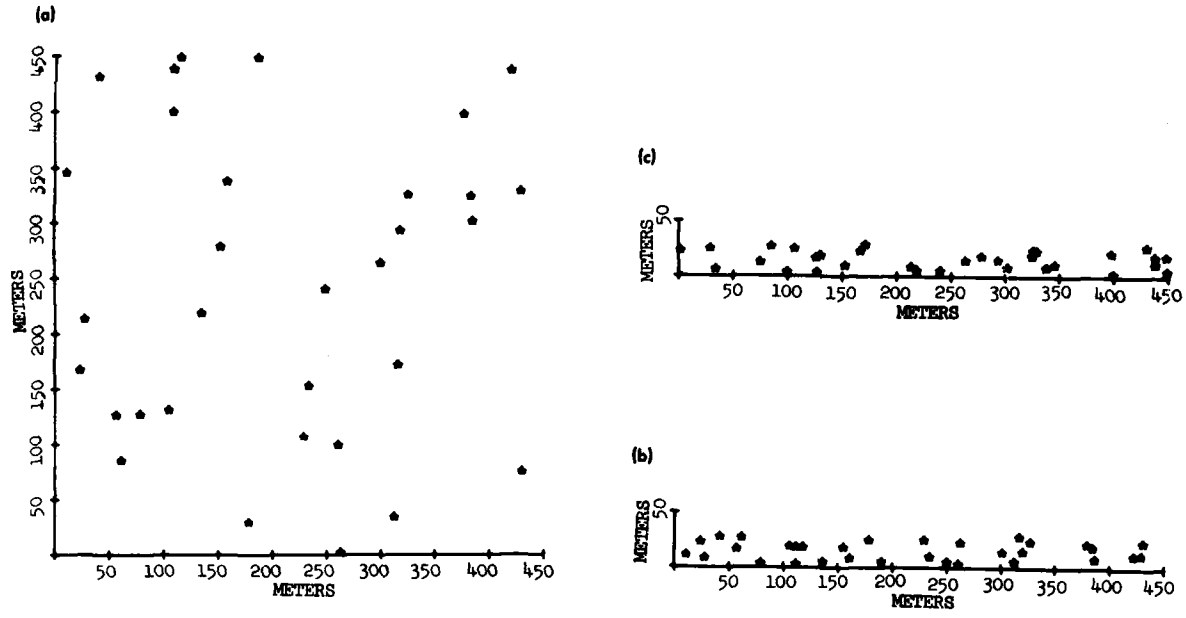

FIG. 5. Random array of 32 elements (a) y versus x, (b) z versus x, (c) z versus y.

more, the patch of solid angle to be investigated typically is neither strictly limited to the horizontal plane nor as large as full angular coverage. Thus the number of beams required in applications of the Dynamic Beamformer would lie somewhere between the bounds indicated in the figure.

C. An example

As a specific example, Fig. 5 shows a single realization of a 32-element, roughly planar, random array. All element locations were assumed independent of one another with identical probability density functions statistically characterizing their individual spatial distributions. Furthermore, the individual distributions were assumed independent and uniform in each dimension of Cartesian coordinates. In this case, array dimensions and frequency are chosen such that $L_x = L_y = 15\lambda$ and $L_z = 1\lambda$. Beam patterns corresponding to these element locations are illustrated in Fig. 6 for an edge-fire beam pointing in the $\theta = \phi = 0°$ direction. The three-dimensional plot has a floor set at $-10 \log N = -15$ dB which is the expected side-lobe level (with respect to a 0 dB on-axis response) for a random array of $N = 32$ elements. Underscoring the statistical nature of the side-lobe structure, note that several side lobes reach levels greater than this mean value.

D. Time-delay quantization

Time domain digital beamforming begins with sampling of the individual sensor signals $e_n(t)$ in (1). With reasonably sharp low-pass filtering of the analog data, sampling need be carried out only slightly above the Nyquist rate (e.g., 2.5 times the maximum frequency of interest) to avoid aliasing or folding out-of-band spectral components down into the baseband of interest. The scalar product in (2) defines the amount each sensor signal ideally should be time-delayed to form a beam in the $\mathbf{B}_m$ direction. The time delays actually available are determined by the data sampling interval. As will be shown below, it is quantization of the time delays which has a far more serious impact on the sensor signal sampling interval than does the Nyquist rate.

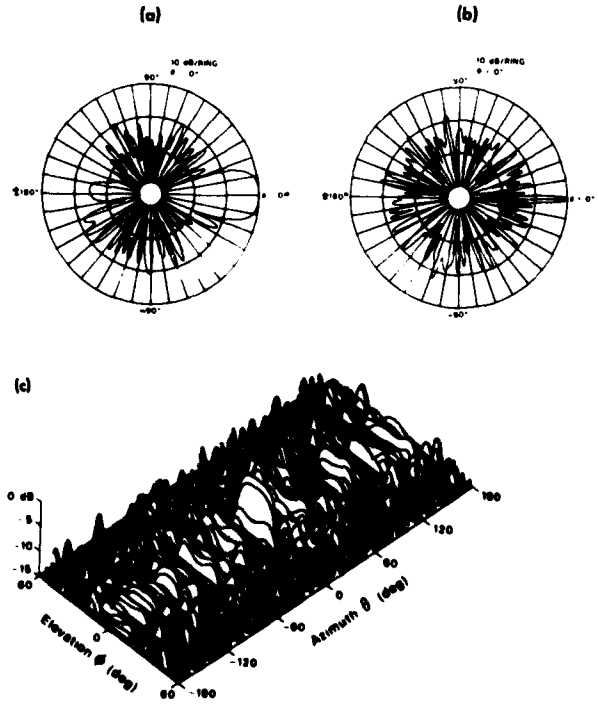

FIG. 6. Random array beam patterns ($\mathbf{B}_m$: $\theta = \phi = 0°$).

With reference to the development in Sec I A, the ideal array spatial transfer function $A_0(\mathbf{u})$ will be defined as the complex transfer characteristic between $s_1(t) = \exp(j\omega t)$ and $b_m(t)$ in the absence of time-delay quantization. Thus

$$A_0(\mathbf{u}) = \sum_{n=1}^{N} \exp\left(-j\omega \frac{\mathbf{E}_n \cdot (\mathbf{B}_m - \mathbf{S}_1)}{c}\right), \tag{4}$$

$$= \sum_{n=1}^{N} \exp(j\mathbf{E}_n \cdot \mathbf{u}), \tag{5}$$

where

$$\mathbf{u} = (\omega/c)(\mathbf{B}_m - \mathbf{S}_1). \tag{6}$$

At a given frequency ω, time-delay quantization has the effect of introducing phasing errors $\delta\phi_n$ into the summation in (5). Incorporating these errors, the actual array spatial transfer function is expressed as

$$A(\mathbf{u}) = \sum_{n=1}^{N} \exp(j\delta\phi_n)\exp(-j\mathbf{E}_n \cdot \mathbf{u}). \tag{7}$$

Assuming the phasing errors to be small, replace $\exp(j\delta\phi_n)$ in (7) by the first two terms of its series expansion $(1 + j\delta\phi_n - \delta\phi_n^2/2 + \ldots)$,

$$A(\mathbf{u}) \simeq \sum_{n=1}^{N} (1 + j\delta\phi_n)\exp(-j\mathbf{E}_n \cdot \mathbf{u}), \tag{8}$$

$$= A_0(\mathbf{u}) + j\sum_{n=1}^{N} \delta\phi_n \exp(-j\mathbf{E}_n \cdot \mathbf{u}). \tag{9}$$

Thus the first-order effect of time-delay quantization is an error term (transfer characteristic) added to the ideal spatial transfer function $A_0(\mathbf{u})$.

In many applications, the magnitude squared value of the spatial transfer function is of primary interest and is generally referred to as the array beam or power pattern. Assuming the $\delta\phi_n$ are zero-mean, identically distributed, and independent of one another, the expected value of the beam pattern is given by[1,3]

$$E[A(\mathbf{u})A^*(\mathbf{u})] = \alpha A_0(\mathbf{u})A_0^*(\mathbf{u}) + N(1-\alpha), \tag{10}$$

where

$$\alpha = |E[\exp(j\delta\phi_n)]|^2. \tag{11}$$

When the phasing errors are uniformly distributed over the interval $-\delta\phi/2 \leq \delta\phi_n \leq \delta\phi/2$, Eq. (11) evaluates to

$$\alpha = \left(\frac{\sin(\delta\phi/2)}{\delta\phi/2}\right)^2. \tag{12}$$

Furthermore, when $\delta\phi$ is sufficiently small to replace the numerator of (12) by the first two terms in its Taylor series expansion

$$\alpha \simeq 1 - (\delta\phi^2/12). \tag{13}$$

Thus the expected value of the beam pattern in (10) can be rewritten as

$$E[A(\mathbf{u})A^*(\mathbf{u})] = \left(1 - \frac{\delta\phi^2}{12}\right)A_0(\mathbf{u})A_0^*(\mathbf{u}) + N\frac{\delta\phi^2}{12}. \tag{14}$$

Note that $\delta\phi/2\pi$ corresponds to the fractional data sampling interval with respect to one cycle at the frequency of interest ω.

Errors due to time-delay quantization can be considered separately in two major regions of the expected beam pattern. First, (14) indicates that when N is large the predominant effect in the direction of desired maximum response ($\mathbf{u} = 0$) is an attenuation from $A_0(0)A_0^*(0) = N^2$ by the factor $(1 - \delta\phi^2/12)$. This on-axis loss is illustrated graphically in Fig. 7 as a function of fractional data sampling interval. Indicated with symbols in the expected degradation at the uppermost frequency of interest in the Dynamic Beamformer (400 Hz) for sensor data sampling rates: (1) 1 kHz (circle), (2) 2 kHz (triangle), and (3) 8 kHz (square).

The second region involves the array side-lobe response. The expected beam pattern in this region con-

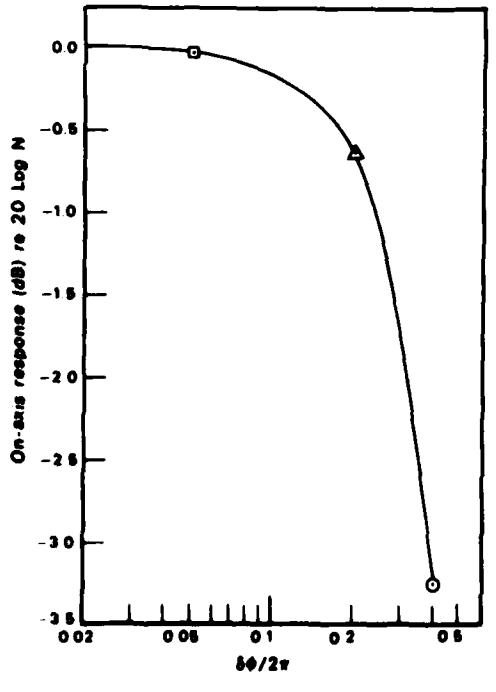

FIG. 7. Time-delay quantization effects.

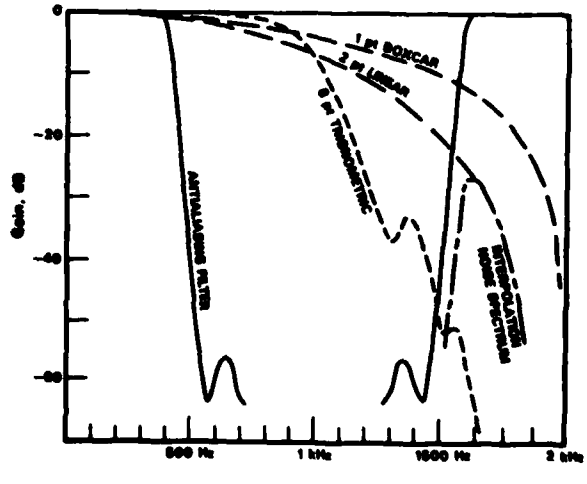

FIG. 8. Antialiasing and interpolation filter response along with the interpolation noise spectrum.

sists of an attenuated version of the side-lobe level in the absence of time-delay quantization effects plus an additive, directionally independent term. Recall that the unnormalized, mean side-lobe level of a random array is N. Thus (14) indicates that time-delay quantization has the average effect of shifting the level of all side lobes towards this mean value.

Since in a random array one has little control over the side-lobe structure due to its statistical nature, the effects of time-delay quantization are of greatest concern in the main-lobe region of the beam pattern. Note from Fig. 7 that in order to preserve an on-axis response to within 0.01 dB of 20 $\log N$ for signals at 400 Hz, a sampling rate of 8 kHz is required.

E. Data interpolation

Since the frequencies of interest to the Dynamic Beamformer lie below 400 Hz, antialiasing considerations alone would suggest that a sampling rate of 1 kHz would be adequate. Figure 8 illustrates the frequency response of the 7 pole, elliptic, low-pass filter used to preprocess the individual analog sensor signals prior to digitization. The replicated spectrum centered on the 2-kHz sampling frequency is well separated by this antialiasing filter. In fact, it is evident that even at a 1-kHz sampling rate there would be minimal overlap or aliasing of the spectra. The discussion in Sec. I D has indicated, however, that is quantization of the beamforming time delays which has the greatest impact on the required interval between samples. A sampling rate of 8 kHz would be desirable to maintain on-axis response to within 0.01 dB of 20 $\log N$ for signals at 400 Hz.

As discussed by others,[6-8] digital interpolation of the sampled sensor signals within the beamformer is one means by which the desired sampling rate can be realized. Essentially, by introducing interpolation hardware into the system, increased complexity of the beamformer hardware is being traded-off against reduced complexity of the sensor signal conditioning hardware, bandwidth requirement of the communication link to the beamformer, and density (or volume) of the storage medium used for data archival.

The process of interpolation involves summing weighted versions of the available data samples both preceding and following the instant in time at which an estimate of the original sensor waveform is desired. The accuracy of the estimate depends on several factors: (1) The sampling rate of the original analog data, (2) the number of samples used to form the estimate, and (3) the values of their corresponding weighting coefficients. Interpolation is quite often viewed as a cascade of two operations. First, zero-valued samples are inserted between the original data samples such that the new sequence occurs at the desired rate. The new sequence then is passed through a low-pass filter to attenuate the periodic replications of the original signal spectrum resulting from the zero-padding operation.[9] This low-pass filter can be implemented as a transversal filter with tap spacings equal to the new sampling interval and tap weights equal to the interpolation coefficients. In the case of the beamformer interpolator, the data rate is not increased. Instead, a sample with a different, interpolated time delay is computed directly for each channel required as input to the beam summation. Once the beam has been formed as indicated in (2), the beam time series sampling rate will be reduced to a value commensurate with the Nyquist rate for the highest frequency of interest. As a result, the attenuated replications of the original single element spectra fold back into the desired low-frequency region of the beam spectrum and can be viewed as interpolation noise.

Considering a sensor signal sampling rate of 2 kHz (twice the rate which would be adequate for the 400-Hz upper cutoff in the Dynamic Beamformer), Fig. 8 illustrates the attenuation characteristics of three candidate interpolation filters.[10] Although the 2-kHz sampling rate is well in excess of that required to insure minimal aliasing of the individual sensor spectra, that frequency was selected to provide sufficient separation of the sensor spectra replications so that a two-point linear interpolator can be used. Linear interpolation involves the simple combination of a single data sample on either side of the desired sampling instant and requires a negligible increase in the complexity of beamformer hardware. The resulting spectral shape of the attenuated, periodic replication of the individual sensor spectrum is identified in Fig. 8 as the interpolation noise spectrum and is seen to have a peak of 28 dB below that of the desired low-frequency region of the beam spectrum.

II. A HARDWARE DYNAMIC BEAMFORMER

In the selection of a particular hardware architecture for a digital time-domain beamformer, a number of interacting considerations come into play. Included are (1) data sampling rate, (2) interpolator design, (3) size of the time-delay memory field, (4) additional memory for block processing, and (5) number of beams to be formed. The particular choices made for the MPL Dynamic Beamformer will be outlined in what follows.

A. Specifications

Specifications for the MPL Dynamic Beamformer are provided in Table I. The impact of time-delay quantization error considerations and interpolation filter complexity is reflected in the selection of a 2-kHz basic

TABLE I. Dynamic Beamformer specifications.

Bandwidth	10–400 Hz
Number of channels	32
Sampling rate	2 kHz
Interpolation-linear	8 kHz
Maximum time delay	2.048 s
Block buffer	6.144 s
Number of beams	1300
Memory	16 KB×32 channel = 500 KB
Data recording	9 Track digital 45 ips 1600 bpi NRZ 10.8 min/2400 ft. Reel

sampling rate which then is interpolated further to an effective 8-kHz rate by the use of a simple linear interpolation operation.

The large number of beams formed in parallel by the Dynamic Beamformer is a consequence of its intended use to process sensor data from a sparsely filled random array. Recall from the discussion in Sec. I B that it is the aperture of the array and not the number of array elements which determines how many beams are required to adequately probe large sectors of space.

In any experimental program, it is almost mandatory that some means of data recording be provided for later off-line analysis. A first impulse might be to record the output of the signal processor. However, in this case, where 32 sensor signals are transformed into 1300 beams, each with the same data rate, 45 times more recording capability would have to be provided in order to store the output rather than the input data. Thus a recording capability for the digitized individual sensor signals has been incorporated into the total system.

A photograph of the Dynamic Beamformer along with its tape deck and communication terminal is given in Fig. 9.

B. Data relationships (input/output)

The structure of data flow into and out of the Dynamic Beamformer is illustrated in Fig. 10. As shown in Fig. 10(a), after signal conditioning the 32 sensor input channels are sampled in parallel (1 byte/sample). Both the element coordinate data and the 32 channels of acoustic data are formated into a basic 36-byte block consisting of a sync byte (FF), and element identifier byte (the value of "n" in Fig. 2), two bytes of element location vector coordinate data (the value of "x," "y," or "z" in Fig. 2), followed by the 32 bytes of sensor data samples corresponding to one instant in time. The resulting 2-kHz frame rate, 36 bytes/frame, ungapped data stream is both sent to the Dynamic Beamformer memory (where it is demultiplexed) as well as recorded continuously on a 9-track, 45 ips magnetic tape drive at a density of 1600 bpi.

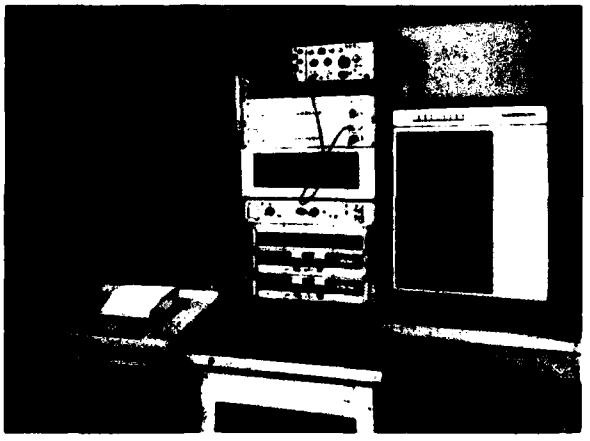

FIG. 9. Photograph of the Dynamic Beamformer tape deck and terminal.

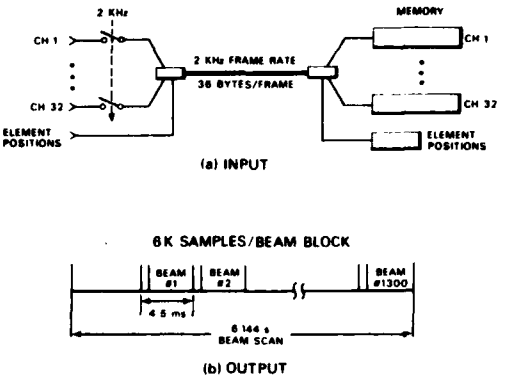

FIG. 10. Data relationships (input/output).

The large memory field provided for each channel in the Dynamic Beamformer enables the formation of beam samples in blocks of 6-K samples/beam ($K = 1024$). As indicated in Fig. 10(b), each block requires 4.5 ms of real time for generation. Although generated at a high data rate in burst sequences, the beam samples correspond to a real-time sampling rate of 1 kHz which is half the original rate for digitization of the sensor signals. The beam blocks are output consecutively with an entire beam can requiring 6.144 s for completion. A continuous sequence of samples corresponding to the mth beam can be obtained by first demutliplexing each beam scan, then concatenating together the mth beam blocks from consecutive beam scans.

C. Channel memory field

For each beam to be formed, time-delayed samples of the array element waveforms are obtained from a continuously updated memory bank which provides a random access signal field. There are two constraints which determine a lower bound on the size of this field. First, sufficient memory must be provided for each element to cover the maximum acoustic travel time across the physical aperture of the array. The dimension D/λ of the array (see Sec. I B) is just the number of wavelengths in the memory field needed to satisfy this requirement. Second, some additional buffer or block storage must be provided. The length of this block memory is determined by the computational burden imposed by the scalar product calculation in (2). The longer the block length, the greater the time available for computing a set of time delays for the next beam to be processed.

These two considerations involved in determining the channel memory field length are portrayed graphically in Fig. 11. The time-delay portion satisfies the first constraint. The cross-hatched areas correspond in length to the block storage portion and represent displaced blocks of memory which contain time-delayed replicas of the sampled element acoustic data. Neglecting interpolation, beamforming as in (2) can be viewed as a simple vertical sum across the displaced memory field.

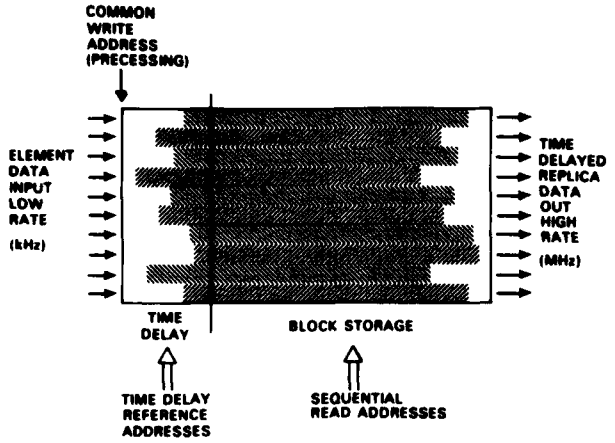

FIG. 11. Channel memory field.

D. Hardware architecture

The basic architecture of the Dynamic Beamformer is shown in Fig. 12. In addition to the 7-pole elliptic low-pass antialiasing filter mentioned previously, the signal conditioning for each channel provides for a common 20-dB gain adjustment and a spectral weighting low-pass filter with selectable cutoff frequencies from 50 to 400 Hz. A bank of sample-and-hold circuits operates synchronously at the 2-kHz sampling rate. The parallel channel amplitude levels are multiplexed, converted to an 8-bit digital sample, then sent on to the data formatter in a serial byte stream. An IEE data bus couples external digital data consisting of array element position and beam vector coordinates into the data formatter. All byte data values are restricted to the range 00–FE (hex) so that FF (hex) can be reserved as a sync byte.

When the tape recorder is running (either in the record or playback mode), the read head output supplies the input to the Dynamic Beamformer. The input is in the form of an 8 bit acoustic data stream to be demultiplexed in the Element Signal Processing modules (one ESP module for every 8 channels), and a sequence of 16-bit element coordinate values and their identifying addresses to be stored in the program control computer.

Beam output samples are formed by summing appropriately delayed and interpolated channel data samples. Multiple beams can be formed since the beam summation process can be carried out faster than the input acoustic data sampling rate. In the Dynamic Beamformer, the time required for the parallel summation across channels is determined by the memory access rate of 3.2 MHz. Comparing this with the 2-kHz acoustic data sampling rate and allowing some system overhead time, approximately 1500 memory accesses are completed in each 0.5-ms input sampling period. The linear interpolation operation requires two samples from memory. However, since the data rate of the beam output samples only needs to be half the original acoustic data sampling rate, 1500 beam samples are generated for each equivalent output sampling period of 1 ms.

The Dynamic Beamformer can accomodate a differential time delay of 2.048 s which corresponds to 4 KB (KB =1024 bytes) of memory per channel. An additional 12 KB of memory per channel corresponding to 6.144 s of input data has been provided for block storage. The additional memory makes available time to carry out the scalar products required in (2). These calculations must be repeated each beam scan for every beam since the array element positions and beam vectors are treated as dynamic variables.

Presettable counters are used as address generators for each channel in the memory field. Each one is preset to a starting address which corresponds to the required time delay for that particular array element. The counters then run synchronously at the 3.2-MHz memory access rate for 12-K samples. Allowing some system overhead time, 4.5 ms is required to generate a time compressed burst of the equivalent of 6.144 s

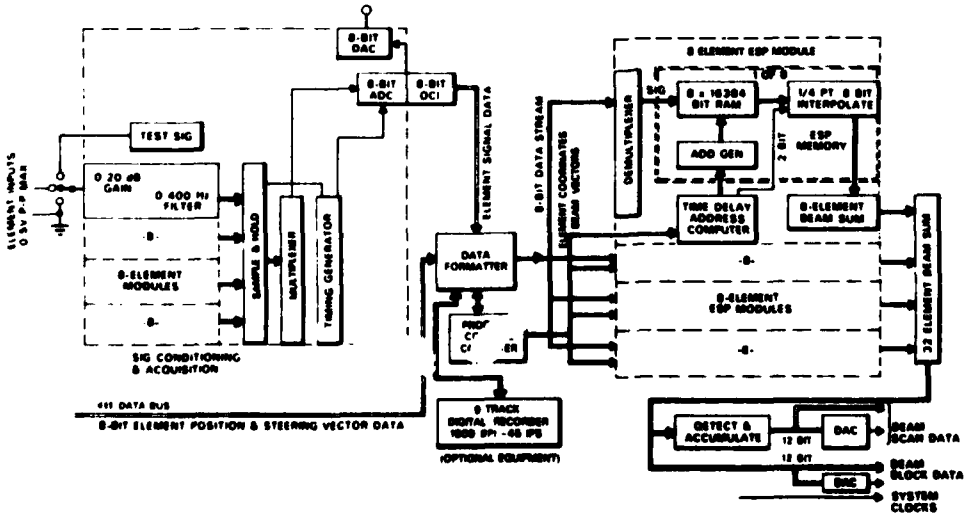

FIG. 12. 32 element Dynamic Beamformer block diagram.

of output data for a single beam sampled at a 1-kHz rate.

During the 4.5 ms interval, four slave microcomputers (one for each ESP module) implement the scalar product in (2) between a new beam vector and a set of element position vectors to generate the time delays for the next beam. Texas Instruments 990/4 16-bit microcomputers were selected for this task. Each 990/4 calculates the time delays for eight elements within the 4.5-ms period. A fifth 990/4 microcomputer augmented by an additional 24 KB of RAM is used as a master controller.

All of the software for the system is resident within the master controller. The element position and beam vector coordinates also are stored there in memory. The scalar product programs are downloaded into the slaves from the master controller over an asynchronous communication link. In the interest of maintaining robust performance in the presence of spurious noise, the slave program memory is reloaded every 6.144 s at the initialization of a new beam scan. This procedure requires 0.294 s and occupies the initial portion of the beam scan graphically portrayed in Fig. 10. In addition, at the beginning of each 4.5-ms beam block, the position vector for one of the eight elements and the vector defining the next beam of the beam scan are downloaded into the slaves.

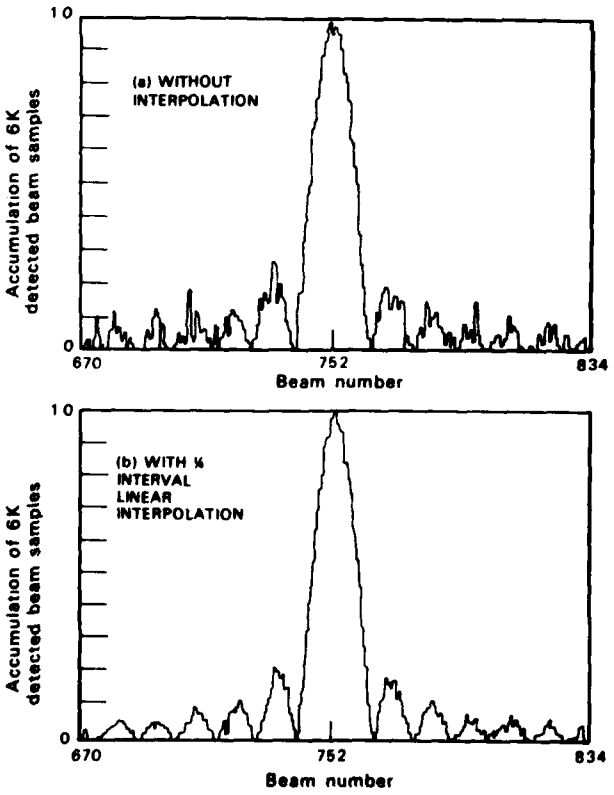

FIG. 13. Dynamic Beamformer bearing response to an 200-Hz broadside test signal.

E. Experimental bearing response

As an aid to check proper operation of the Dynamic Beamformer, provision has been made to input an externally supplied signal to all channels simultaneously. Thus the reception of a broadside arrival by a line array of elements can be simulated.

With a test signal frequency of 200 Hz, detected beam scans resulting when the sensor locations of a 16-element array uniformly distributed along the x axis were loaded into memory are shown in Fig. 13. Array element spacing was 14 ms in terms of time delay which is slightly less than 3λ at this frequency. From left to right in Fig. 13 for this expanded segment of a 1024 beam set, azimuth values (see Fig. 2) start at approximately 83°, pass through 90° (broadside beam) half-way across the figure, and stop at approximately 97°. Each beam is represented by a single point derived by absolute value detecting and accumulating the 6-K beam output samples across an entire beam block (see Fig. 12).

Figure 13 compares the test signal bearing response prior to and after the incorporation of linear interpolation into the hardware. All distortions from a smooth response as a function of azimuth in Fig. 13 are a result of time-delay quantization and are exactly reproducible. Note the significant improvement of the sidelobe response with the addition of $\frac{1}{4}$-interval linear interpolation.

III. DATA ANALYSIS FLEXIBILITY

A number of features have been incorporated into the Dynamic Beamformer which provide a great deal of flexibility during data analysis. Of primary significance is the capability to interact with the master controller on a real-time basis and thus alter the mode of operation. For example, the master controller issues commands to the magnetic tape recorder calling for forward, fast forward, rewind, or stop. Since this interaction can be with another computer as opposed to an operator, a closed-loop mode of data analysis is possible, where the second computer monitors the output of the Dynamic Beamformer and alters its operation based on what has been learned about the data.

Several specific features which have proven useful include:

(1) Element masking (selectively turning off any one or group of channels),

(2) freezing data in memory (successive beam scans work with identical data),

(3) real-time modification of element locations and beam vectors,

(4) outputting both the actual beam samples as well as the result of absolute value detecting, then accumulating the entire beam block (the second yields a measure of broadband energy in 6.144 s),

(5) outputting the individual array element samples as the first 32 "beams" (provides a means by which array signal gain and array gain calculations can be made easily),

(6) allowing beam scan reference (starting beam), width (number of beams to output prior to initiating a new beam scan), and dwell (number of consecutive beam blocks to be output which will correspond to the same beam) to be variable.

IV. CONCLUSIONS

The design considerations and hardware architecture of a programmable, time domain, digital beamformer built by MPL has been discussed. The hardware has proven effective in the analysis of data from a sonobuoy thinned random array. Although the hardware which was built is limited to processing 32 sensor channels, the beamformer architecture is amenable to expansion in modules of 8 channels per module.

ACKNOWLEDGMENTS

This work was sponsored by the Office of Naval Research, contract N00014-75-C-0749. The hardware fabrication was carried out by W. R. Cherry of the Marine Physical Laboratory.

[1]M. I. Skolnik, "Nonuniform Arrays," in *Antenna Theory*, edited by R. E. Collin and F. J. Zucker (McGraw-Hill, New York, 1969) pp. 207-234.
[2]Y. S. Shifrin, *Statistical Antenna Theory* (Golem, Boulder, CO, 1971).
[3]B. D. Steinberg, *Principles of Aperture and Array System Design* (Wiley, New York, 1976).
[4]J. V. Thorn, N. O. Booth, and J. G. Lockwood, "Random and partially random acoustic arrays," J. Acoust. Soc. Am. 67, 1277-1286 (1980).
[5]W. S. Hodgkiss, "Random Acoustic Arrays," NATO Advanced Study Institute on Underwater Acoustics and Signal Processing, 18-29 August 1980, Copenhagen, Denmark.
[6]R. G. Pridham and R. A. Mucci, "A novel approach to digital beamforming," J. Acoust. Soc. Am. 63, 425-433 (1978).
[7]R. G. Pridham and R. A. Mucci, "Digital interpolation beamforming for low-pass and bandpass signals," Proc. IEEE 67, 904-919 (June 1979).
[8]R. G. Pridham and R. A. Mucci, "Shifted sideband beamformer," IEEE Trans. Acoust. Speech, Signal Process. ASSP-27, 713-722 (December 1979).
[9]A. Peled and B. Liu, *Digital Signal Processing* (Wiley, New York, 1976).
[10]V. C. Anderson, "Efficient computation of array patterns," J. Acoust. Soc. Am. 61, 744-755 (1977).

ONR/MPL GENERAL DISTRIBUTION LIST

Chief of Naval Research
Department of the Navy
Arlington, Virginia 22217
Code 200, 220(2), 102C, 460

Naval Ocean Research
and Development Activity (NORDA)
Chief of Naval Research Detachment
NSTL Station
Bay St Louis, Mississippi 39529
Code 420, 421, 424

Director
Office of Naval Research
Branch Office
1030 East Green Street
Pasadena, California 91101

Commander
Naval Sea Systems Command
Washington, D C 20362
Code 63, 63R, 63R-23

Defense Advanced Res Proj Agency
1400 Wilson Boulevard
Arlington, Virginia 22209
Atten CDR Vernon P Simmons

Commander
Naval Air Systems Command
Washington, D C 20361
Code 370, 264

Commander
Naval Ship Res & Dev Center
Bethesda, Maryland 20084

Director
Strategic Systems Proj Ofc (PM-1)
Department of the Navy
Washington, D C 20361
Code NSP-2023

Commander
Naval Surface Combat Systems Center
White Oak
Silver Spring, Maryland 20910

Commanding Officer
Civil Engineering Laboratory
Naval Construction Battalion Center
Port Hueneme, California 93043
Code L40, L42

Deputy Commander
Operation Test & Evaluation
Force Pacific
U S Naval Air Station
San Diego, California 92135

Director of Research
U S Naval Research Laboratory
Washington, D C 20375
Code 2620, 2627, 5000, 5100, 5800

Commanding Officer
Naval Coastal Systems Laboratory
Panama City, Florida 32401

Director
Defense Documentation Center
(TIMA), Cameron Station
5010 Duke Street
Alexandria, Virginia 22314

Commanding Officer
Naval Ocean Research and
Development Activity (NORDA)
NSTL Station
Bay St Louis, Mississippi 39529
Code 100, 110, 300, 330,
340, 350, 360, 500

Commander
U S Naval Oceanographic Office
NSTL Station
Bay St Louis, Mississippi 39522
Bill Jobst

Commander
Submarine Development Group ONE
Fleet Post Office
San Diego, California 92152

Commander
Naval Electronics Systems Command
Washington, D C 20360
Code PME-124, 320A

Commanding Officer
U S Naval Air Development Center
Attention Jim Howard
Warminister, Pennsylvania 18974

Officer in Charge
Naval Ship Research & Dev Center
Annapolis, Maryland 21402

Commander
Naval Ocean Systems Center
San Diego, California 92152
Code 52, 531 5301,
71, 72, 614

Commanding Officer
Naval Underwater Systems Center
Newport, Rhode Island 20f44
Atten John D'Albora

Officer in Charge
Naval Underwater Systems Center
New London Laboratory
New London, Connecticut 06320
Code 900, 905, 910, 930, 960

Executive Secretary, Naval Studies
Board
National Academy of Sciences
2101 Constitution Avenue, N W
Washington, D C 20418

Assistant Secretary of the Navy
(Research Engineering & Systems)
Department of the Navy
Washington, D C 20350

STOIAC
Battelle Columbus Laboratories
505 King Avenue
Columbus, Ohio 43201

National Oceanic & Atmospheric
Administration
Ocean Engineering Office
6001 Executive Boulevard
Rockville, Maryland 20852

Institute for Defense Analyses
400 Army-Navy Drive
Arlington, Virginia 22202

Chief Scientist
Navy Underwater Sound Reference Div
U S Naval Research Laboratory
P O Box 8337
Orlando, Florida 32806

Supreme Allied Commander
U S Atlantic Fleet
ASW Research Center, APO
New York, New York 09019
Via ONR 210, CNO OP092D1,
Secretariat of Military,
Information Control, Committee

Director
College of Engineering
Department of Ocean Engineering
Florida Atlantic University
Boca Raton, Florida 33431

Director
Applied Research Laboratory
Pennsylvania State University
P O Box 30
State College, Pennsylvania 16802

Director
Inst. of Ocean Science & Engineering
Catholic University of America
Washington, D C 20017

Director
Lamont-Doherty Geological Observatory
Torrey Cliff
Palisades, New York 10964

Director
The Univ of Texas at Austin
Applied Research Laboratory
P O Box 8029
Austin, Texas 78712

Director
Woods Hole Oceanographic Institution
Woods Hole, Massachusetts 02543

National Science Foundation
Washington, D C 20550

Superintendent
U S Naval Postgraduate School
Monterey, California 93940

Director
Atten Dr J Robert Moore
Institute of Marine Science
University of Alaska
Fairbanks, Alaska 99701

Director
Applied Physics Laboratory
Johns Hopkins University
Johns Hopkins Road
Laurel, Maryland 20810
Atten J R Austin

Director
Marine Research Laboratories
c/o Marine Studies Center
University of Wisconsin
Madison, Wisconsin 53706

Director
Applied Physics Laboratory
University of Washington
1013 East 40th Street
Seattle, Washington 98105

University of Rochester
Center of Naval Analysis
1401 Wilson Boulevard
Arlington, Virginia 22202

Meterological & Geo-Astrophysical
Abstracts
301 East Capitol Street
Washington, D C 20003

Office of Naval Research
Resident Representative
c/o Univ of California, San Diego
La Jolla, California 92093

University of California, San Diego
Marine Physical Laboratory Branch Office
La Jolla, California 92093

January 1981

END

DATE
FILMED

1-82

DTIC